Melt movement and the occlusion of porosity in crystallizing granitic systems

D. N. BRYON, M. P. ATHERTON, M. J. CHEADLE AND R. H. HUNTER

Department of Earth Sciences, University of Liverpool, Liverpool, L69 3BX, UK

Abstract

Porosity occlusion has been studied in a granodiorite rock from the Peruvian Coastal Batholith. The texture of the granodiorite is characteristic of Cordilleran I-type rocks, and the textural relations and modelled crystallization path within the quaternary An–Ab–Or–Qz system indicate alkali feldspar was the last major phase to start crystallizing. In thin section, alkali feldspar crystals occur both as large anhedral 'plates' containing numerous inclusions, and small interstitial cuneiform 'pockets'. The alkali feldspar pockets are interpreted as late stage nucleation and growth of new crystals in pores that became isolated from the larger crystals during the latter stages of crystallization. Their geometry therefore mirrors that of the pores immediately after isolation.

From the modal abundance of the interstitial pockets, and taking into account contemporaneous growth of the other major phases, it is suggested that crystallization in isolated pores involved solidification of the final 3–4% of liquid. Alkali feldspar growth on the rims of the large anhedral plates prior to pore isolation is evidence for the localised (mm-cm scale) diffusion of chemical species within the interconnected melt phase. However, Rayleigh number calculations indicate that the separation of melt from crystals by compositional convection is unlikely to have occurred during interstitial crystallization.

KEYWORDS: granite, textural development, porosity occlusion, compositional convection.

Introduction

Many granitic intrusions are compositionally zoned, usually from a mafic margin/bottom to a more evolved felsic core/top. Much modal and chemical data exist on such bodies and, in many cases, compositional variation has been explained by fractional crystallization from a single parent magma (e.g. Ragland and Butler, 1972; McCarthy and Robb, 1978; Tindle and Pearce, 1981). Implicit in any fractionation model is that melt and crystals move relative to one another. The removal of early-formed crystals from the melt in siliceous systems by crystal settling is not now thought to dominate this process, and recent experimental and theoretical advances in the field of fluid dynamics have highlighted the possible importance of buoyancy driven removal of lighter, more evolved melt from boundary layers surrounding growing crystals (e.g. Sparks *et al.*, 1985; Martin, 1990; Tait and Jaupart, 1992; Petford, 1993). This process has been cited in several recent field-based studies of granitic bodies to explain the evolution of macroscopic compositional zonation (Sawka *et al.*, 1990; Mahood and Cornejo, 1992). However, it is still unclear how the microscopic movement of melt relates to textural development during the three main stages of crystallization in granitic magma systems (Fig. 1). Is movement restricted to high melt fractions before the system develops a continuous crystal framework, or does it continue after framework development, with melt channelled through the interstitial pores? In the latter case, at what melt fraction does the pore volume become sufficiently reduced to induce the breakdown of an interconnected porosity and so restrict movement, and what criteria can be used to identify and quantify the transformation from the solidified texture?

In many ways the problem is comparable to porosity occlusion, and its effect on permeability, in sedimentary systems. However, unlike sediments, criteria for identifying and quantifying pore geometries from crystallized granitic rocks have yet to be developed. This largely reflects problems in

Mineralogical Magazine, February 1996, Vol. 60, pp. 163–171

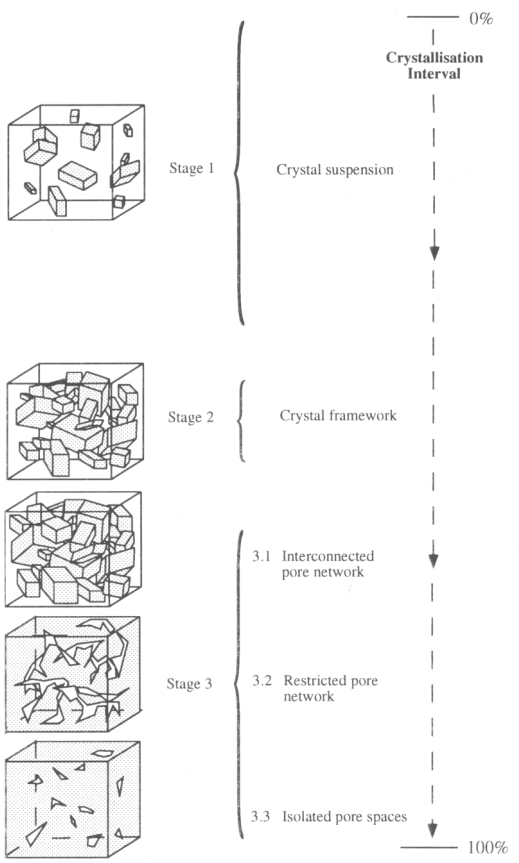

FIG. 1 (modified from Fig. 4 in Bryon *et al.*, 1994). Schematic representation of the sub-division of the crystallization interval into three main stages, namely: crystal suspension (1), crystal framework (2); and interstitial crystallization (3). Interstitial crystallization has been further sub-divided based on the changing relationship between the crystallized products and the interstitial melt during late stage solidification. This interpretation indicates that the pore network progressively changes from interconnected to isolated as the volume of remaining melt decreases.

extracting information about the early evolution of the texture from the solidified rock, and the fact that studies of igneous textures are generally restricted to thin section (presenting little more than a two-dimensional surface through a three-dimensional texture). In addition, recognition of porosity at a given stage of crystallization requires a textural marker that records the pore geometry. Such markers are not obvious in granitic rocks, as crystallization in pore spaces commonly occurs on the rims of early-formed crystals (e.g. Bryon *et al.*, 1994).

Here we present results from an ongoing study of textural development in a suite of granitic rocks from the zoned Linga superunit of the Coastal Batholith of Peru (see Atherton and Sanderson, 1985, for an overview of compositional variation in the Batholith). In this contribution, we concentrate on a single granodiorite sample that shows textural evidence for crystallization in isolated pore spaces during the latter stages of solidification. The melt fraction at which the pore network became discontinuous is estimated from the modal abundance of material that crystallized in the isolated pore spaces. The possibility that compositional convection occurred while the pore network remained open is also addressed.

The texture of the Yauca granodiorite

The granodiorite sample that constitutes the basis of this study shows a characteristic primary Cordilleran mineralogy and texture (Fig. 2), with plagioclase, quartz, alkali feldspar, amphibole and biotite as the major phases, and clinopyroxene, magnetite, apatite and zircon appearing as accessories. The plagioclase crystals are mainly subhedral, and form a touching framework in three dimensions (Bryon *et al.*, 1995). Alkali feldspar forms large anhedral poikilitic plates up to 8 mm in diameter (Fig. 2*b*). These contain unorientated inclusions of all the other major phases. The inclusions do not touch, and appear to have been isolated from the melt before development of a continuous crystal framework. In addition to the poikilitic plates, alkali feldspar forms small anhedral cuneiform 'pockets' that are never larger than 500 μm. Quartz crystals range in geometry from anhedral in the interstices of the plagioclase framework, to equant subhedral crystals whose growth was less restricted. A similar range of geometries is shown by amphibole and biotite, indicating continued growth of both phases through much of the crystallization interval.

The crystallization history of the granodiorite, as deduced from the textural relations and the predicted pathway of the melt in the quaternary An–Ab–Or–Qz system (Fig. 7 in Bryon *et al.*, 1995), is shown in Fig. 3. Plagioclase dominated the early part of crystallization and contributed substantially to the formation of the crystal framework. Amphibole, biotite, quartz and finally alkali feldspar started crystallizing before a continuous crystal framework had been established, and therefore had contributory roles in its development. Contemporaneous crystallization of all the phases after framework formation

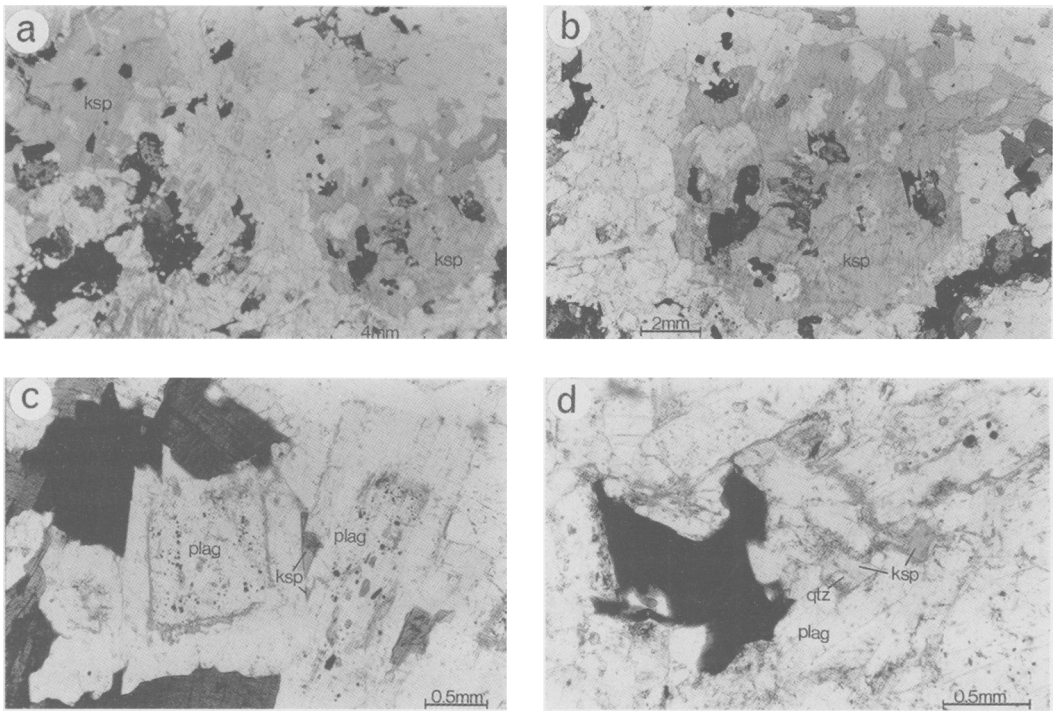

FIG. 2. Plane polarized light photomicrographs of the texture of the Yauca granodiorite from the Peruvian Coastal Batholith. (*a*) General view showing plagioclase dominating the crystal framework along with crystals of amphibole, biotite, quartz and alkali feldspar. (*b*) Example of one of the large alkali feldspar 'plates' containing inclusions of the other major phases. Note the anhedral margin. (*c,d*) Examples of the small cuniform alkali feldspar pockets that lie in the interstices of the crystal framework. One of the pockets in (*d*) contains a small quartz inclusion (arrowed).

occurred primarily by overgrowth on the rims of existing framework crystals.

Alkali feldspar crystallization

The unusual feature about alkali feldspar in the Yauca granodiorite is the clear textural distinction between the large anhedral plates and the small interstitial pockets. This distinction becomes even more evident when the texture is studied in three dimensions using serial thin-sectioning, image analysis, and three-dimensional reconstruction (described in Bryon *et al.*, 1995). The large anhedral plates can invariably be traced through consecutive sections (Fig. 4). The three large plates in the first section shown in Fig. 4 are present in all five subsequent thin sections, indicating minimum 'depths' of 2.5 mm (500 μm between individual sections). The largest crystal (labelled 1) is continuous through a further four sections and is estimated to have a total depth in excess of 5 mm. All of the plates show anhedral margins, and contain suspended inclusions of the other major phases, indicating growth from before framework development to late in the crystallization interval (probably to completion).

In contrast, the interstitial pockets are much smaller and far more abundant (Fig. 4). Individual pockets are only ever present in a single section and therefore have a maximum depth of 500 μm (this is the minimum sectioning distance using this technique). They are generally located well away from the rims of the larger plates, and commonly form localized clusters midway between neighbouring plates (e.g. sections 1 and 4 in Fig. 4). Individual pockets within these clusters characteristically form separate alkali feldspar crystals that extinguish in different orientations (e.g. Fig. 2*d*). The pockets do not appear to be interconnected in three dimensions, and their late-stage interstitial nucleation and growth may therefore have occurred within a restricted or discontinuous pore network (c.f. stages 3.2/3 in Fig. 1).

On the basis of the two- and three-dimensional textural evidence described above, it is suggested that

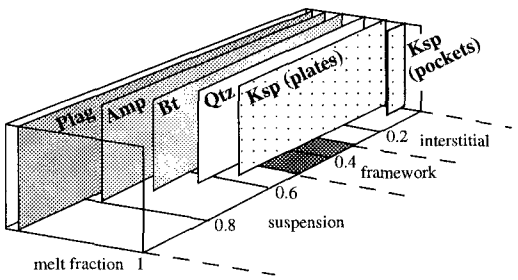

FIG. 3. The crystallization history of the major phases in the Yauca granodiorite as determined from the textural relations and melt pathway in the quaternary An–Ab–Or–Qz system (discussed in detail in Bryon *et al.*, 1994). All the phases started to crystallize during stage 1 (crystal suspension) and hence contributed towards framework development. The division of alkali feldspar into two stages is based on the textural distinction between the large plates and the small pockets.

melt from which the Yauca granodiorite crystallized underwent two separate episodes of alkali feldspar nucleation (Fig. 3). The first of these occurred as the melt evolved to the An–Ab–Or–Qz cotectic before framework development, and resulted in the growth of the large plates. The second stage of nucleation occurred much later in the crystallization interval when the pore network had become discontinuous, and resulted in the growth of the small interstitial pockets. It is suggested that this second stage of nucleation and growth was necessary for alkali feldspar to continue crystallizing within pore spaces that became isolated from the margins of existing plates (c.f. stage 3.3 in Fig. 1). In this respect, the crystallized pockets provide information on both the geometry of isolated pores, and the melt fraction at which the pore network became discontinuous.

Evidence supporting the contemporaneous growth of the late-stage pockets and the rims of the larger plates can be seen by comparing their barium concentrations (Fig. 5). The plates show normal barium zonation, with highest concentrations in the core (maximum of 2.29 wt.% BaO) and the lowest towards the rims (minimum of 0.61 wt.% BaO). Barium concentrations from three separate interstitial pockets are also shown in Fig. 5 (it was impossible to obtain more than two analyses from each pocket, or work on more than three pockets, because of their small size and the difficulty in locating them in unstained sections). All of the concentrations from the pockets are low, and range between 0.84 and 0.66 wt.% BaO. These values are similar to those found towards the rims of the plates, and indicate that the interstitial pockets and the margins of the larger plates grew contemporaneously from a melt of the same composition.

Interpretation of porosity occlusion

Evidence from both the texture and the predicted crystallization pathway in the quaternary An–Ab–Or–Qz system (Fig. 7*a* in Bryon *et al.*, 1995) indicates that the Yauca granodiorite evolved to the cotectic during stage 1 of the crystallization interval, i.e. before the development of a continuous crystal framework. Subsequent contemporaneous growth of plagioclase, quartz and alkali feldspar continued through framework development and interstitial crystallization. It is suggested that while the interstitial melt remained interconnected, growth of plagioclase, quartz and alkali feldspar continued on the rims of existing crystals (Fig. 6*a*). In the case of alkali feldspar, this involved overgrowth of the plates that nucleated before framework development. Continued crystallization led to a reduction of the pore volume and, consequently, the interconnectivity of the interstitial melt (c.f. stage 3.2/3 in Fig. 1). The nucleation and growth of the late-stage interstitial alkali feldspar pockets is interpreted as representing crystallization in melt pockets that became isolated from the larger plates late in the crystallization interval (Fig. 6*c,d*).

Contemporaneous crystallization of plagioclase and quartz during porosity occlusion is interpreted as having occurred on the rims of existing crystals bounding isolated pores. Crystals of both phases are far more abundant than alkali feldspar in the rock, and all the pockets studied are bounded by plagioclase and quartz crystals. The presence of a small quartz inclusion <100 μm across within one of the alkali feldspar pockets (arrowed in Fig. 2*d*) may represent the very late stage growth of a new quartz crystal within an isolated pore, or merely a projection from a marginal crystal not visible in this two-dimensional section.

Quantification of pore isolation

On the assumption that the nucleation and growth of the alkali feldspar pockets marks the breakdown in pore interconnectivity in the Yauca granodiorite, the modal abundance of the pockets can be used to estimate the melt fraction at which pore isolation occurred. However, it is important to remember that alkali feldspar was not the only phase crystallizing, and any estimate should also take into account contemporaneous crystallization of the other major phases.

The late-stage alkali feldspar pockets form only 0.4% by mode of the rock (c.f. 14.5% for the alkali

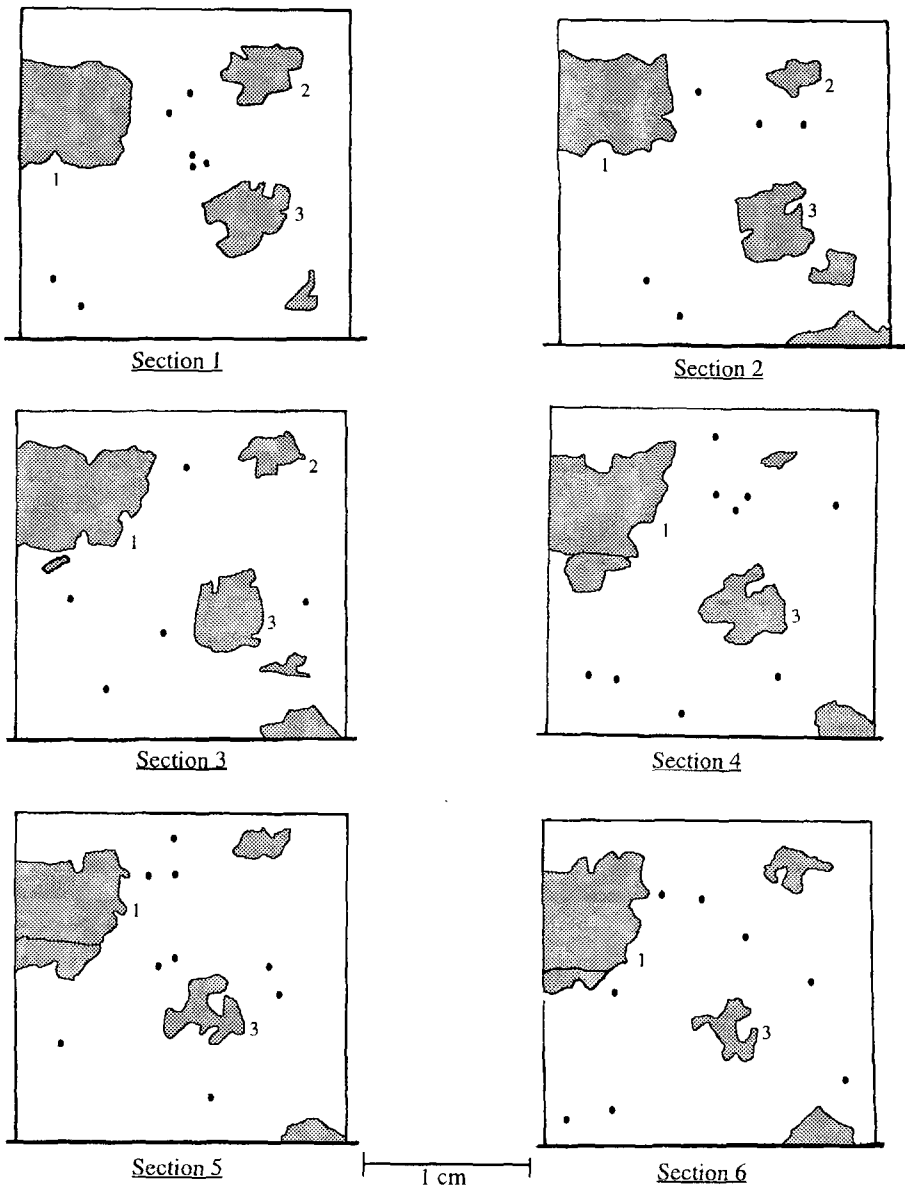

FIG. 4. Variation in the geometry and location of the alkali feldspar plates (shaded grey) and pockets (shown as black dots) through six serial sections from the Yauca granodiorite. The sectioning and digitizing technique is described at length in Bryon *et al.* (1995). The distance between each of the sections is approximately 500 μm. The plates can be traced through consecutive sections, whereas the pockets only ever appear in a single section.

feldspar plates). It is suggested, therefore, that 0.4% of alkali feldspar crystallization occurred in pore spaces isolated from the rims of the existing plates. An estimate of the amount of contemporaneous crystallization of plagioclase and quartz in isolated pore spaces is difficult because there is little evidence preserved in the texture (interstitial crystallization of both phases occurred principally by overgrowth on

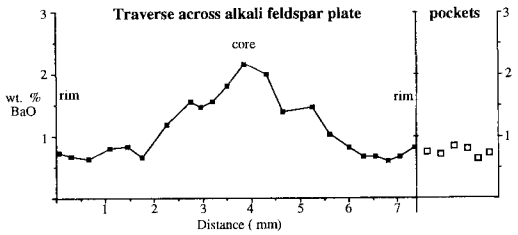

FIG. 5. Barium zonation in a representative alkali feldspar plate and various analyses from the small interstitial pockets. All the plates show a normal zoning trend with highest concentrations in the core and lowest towards the rims. The pockets have values similar to the rims of the plates. All analyses were determined on a CAMECA Camebax EPMA using SPECTA WDS and EDS analysis and on line Link Systems ZAF-4/FLS software packages. The operating conditions were: 15 kV electron beam accelerating potential, 40° take-off angle, 3 μm, 3 nA beam current (for EDS) and 14.5 nA beam current (WDS).

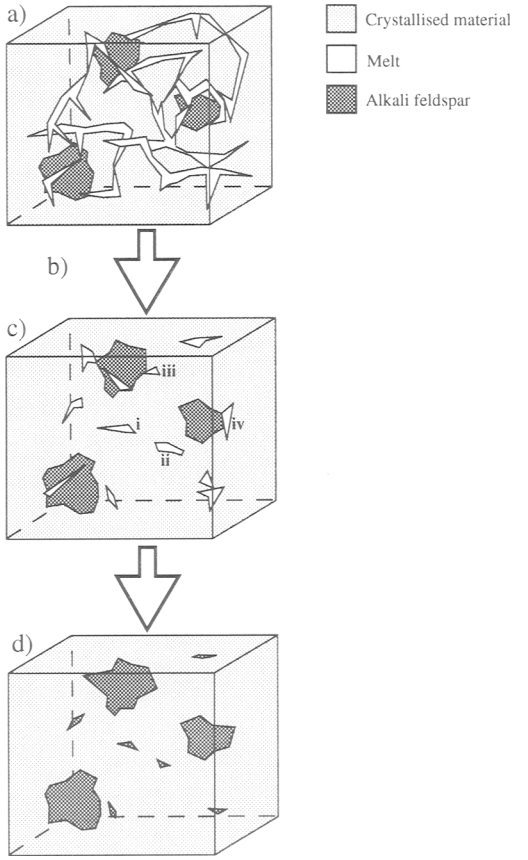

FIG 6. Schematic representation of the change in the connectivity of the pore network in the Yauca granodiorite, and its effect on the crystallization of alkali feldspar. (*a*) Interconnected pore network (c.f. stage 3.1 in Fig. 1). Alkali feldspar crystallization continuing on the rims of the existing 'plates'. (*b*) Continued crystallization leads to a complete breakdown in the connectivity of the pore network. (*c*) Isolated pore spaces (stage 3.3 in Fig.1) containing melt of cotectic composition. Nucleation and growth of new alkali feldspar crystals in isolated pore spaces not in contact with the existing plates (e.g. pores i and ii). Continued crystallization on rims of the plates from pores in contact with plates (e.g. pores iii and iv). (*d*) Final solidified texture showing large anhedral plates and late stage interstitial pockets.

the rims of existing crystals bounding isolated pore spaces). For the purposes of this estimation we have assumed a cotectic growth ratio for the three felsic phases of 1:1:1 (estimated from the position of the cotectic in the An:Ab:Or:Qz quaternary system). Crystallization of plagioclase, quartz and alkali feldspar is therefore interpreted as representing 1.2% of the rock (0.4% of each phase). In addition to the felsic phases, we must also consider contemporaneous late-stage crystallization of the two mafic phases. Both amphibole and biotite crystals show anhedral, occasionally interstitial geometries, and are interpreted as having continued to crystallize through the latter stages of crystallization (Fig. 3). For the purposes of this estimation, we will assume that both phases had similar growth rates to the felsic phases (based on their modal abundance and crystallization histories) and therefore account for 0.8% of crystallization in isolated pores.

So far we have estimated that 2% of crystallization in the Yauca granodiorite occurred in pore spaces isolated from the rims of the large alkali feldspar plates (e.g. pores i and ii in Fig. 6). However, this estimate does not take into account isolated pores in contact with the plates (e.g. pores iii and iv in Fig. 6). Identification and quantification of these is impossible because post-isolation growth of alkali feldspar continued on the rims of the existing plates and therefore no new crystals nucleated. Our estimate of 2% as the total amount of crystallization in isolated pores must therefore be regarded as a minimum. It is more likely, taking into account the abundance and distribution of the plates, that the total will be higher by a factor of 1–2, i.e. approximately 3–4%. This is still very low, and implies that the melt phase in the Yauca granodiorite was interconnected and conse-

quently 'open' for almost all of the crystallization interval.

In texturally equilibrated static systems comprising solid and melt, the melt-filled porosity will always be interconnected if the solid-solid-melt contact angles (dihedral angles) are <60°, no matter what the melt fraction (Smith, 1948; Beere, 1975; Bulau *et al.*, 1979; Hunter, 1987). Melt in systems with dihedral angles >60° will form isolated pockets. This principle is commonly used in studies of melt interconnectivity in basic and ultrabasic systems, where dihedral angle values often lie in the 30–50° range (e.g. Hunter, 1987; Daines and Richter, 1988; Harte *et al.*, 1993).

The few experimental determinations of dihedral angles in granitic systems yield values in the 40–60° range (Jurewicz and Watson, 1985; Laporte, 1988). These results indicate that providing textural equilibrium is achieved, the melt phase in granitic systems should form an interconnecting network throughout crystallization. However, the experiments cannot be directly related to this current study because the Yauca granodiorite shows little evidence of an approach to local textural equilibrium. Therefore the pore system microgeometry during crystallization was not governed by minimisation of grain interface energies.

Compositional convection

The observation that the pore network remained at least partially interconnected down to a porosity of 3–4% raises the question of whether the melt phase moved relative to the crystalline framework during interstitial crystallization. All alkali feldspar growth before pore isolation occurred on the plates, however, the plates themselves are not interconnected in three dimensions. There must, therefore, have been some localised mm-scale movement of melt (or species within the melt) between neighbouring plates.

The driving force for melt movement in a porous mush is the density difference between the lighter evolved interstitial melt and the heavier undifferentiated melt bordering the crystal mush. This fluid motion is termed compositional convection (see review by Huppert, 1990). However, compositional convection will only occur if the destabilizing influence of the compositional buoyancy exceeds the stabilizing influence of the forces that oppose motion. The dimensionless quantity which is the ratio of these two forces is the Rayleigh number. Compositional convection will occur if the porous medium (mush) Rayleigh number (Ra_m) (eqn. 1) (Worster, 1991) exceeds ~25–50 (Fowler, 1985; Tait and Jaupart, 1992).

$$Ra_m = \frac{g\Delta\rho_{(s)}kH}{\kappa\mu} \qquad (1)$$

where g is the acceleration due to gravity, $\Delta\rho_{(s)}$ is the density difference driving compositional convection, k is the permeability, H is the thickness of the mush, μ is the fluid viscosity and κ is the thermal diffusivity.

An estimate of the likely composition of the interstitial melt in the Yauca granodiorite is given in Table 1 (the bulk composition of the sample is also given). This estimate is based on the relative proportions of each of the major phases crystallizing during porosity occlusion as deduced from the textural and phase relations (Fig. 3). Average mineral compositions for each phase were used (Bryon, 1992). The largest uncertainty is in the water content of the melt, and consequently two values were considered (1.5 wt.% H_2O and 6 wt.% H_2O); the larger value representing the possibility that water may be concentrated into the residual melt during the latter stages of crystallization. Appropriate values for the other parameters in the equation are also given in Table 1.

Even using the most optimistic values in equation 1 (i.e. high $\Delta\rho(s)$, large H, and low μ), generates Rayleigh numbers in the range 0.02–0.06. These values are considerably smaller than the critical range of 25–50 required for compositional convection. Based on this evidence, it seems unlikely that significant compositional convection could have occurred within the crystallizing mush of the Yauca granodiorite even though the pore network remained interconnected down to low porosities.

The textural variation of the alkali feldspars in the Yauca granodiorite is probably therefore a consequence of the ability of the crystal species to diffuse through the melt to preferential sites of growth (i.e. the pre-existing large alkali feldspar plates) whilst the porosity network remained open. The three-dimensional distribution and spacing of the plates indicates a maximum length-scale for diffusion of 1 cm. Once the network broke down, the alkali feldspar components within the melt became isolated from plates, and hence new alkali feldspar crystals nucleated and grew within the isolated pores.

Conclusions

Unlike the textures found in many mafic and ultramafic rocks, true interstitial/post-framework phases are commonly absent from granitic textures. Consequently, identification and interpretation of porosity occlusion in granitic rocks is generally impossible because most of the late stage crystallization is 'lost' on the rims of early-formed crystals. This is most noticeable in compositionally evolved granitic rocks, in which the melt crystallized on the cotectic through much of the crystallization interval, resulting in a relatively equigranular mosaic of feldspar and quartz crystals.

TABLE 1. Major element chemistry of the Yauca granodiorite from the Linga superunit of the Peruvian Coastal Batholith. The bulk composition of the rock is shown along with the estimated composition of the interstitial melt after framework development. The interstitial melt composition was calculated from average mineral compositions from the Yauca granodiorite (Bryon, 1992), on the basis of a crystallization ratio by volume of: 0.25 plagioclase: 0.25 quartz: 0.25 alkali feldspar: 0.125 amphibole: 0.125 biotite. This ratio was deduced from textural relations and the predicted pathway within the quaternary An–Ab–Or–Qz system. Viscosities and densities were calculated using the methods of Shaw (1972) and Bottinga *et al.* (1983) respectively. The mush is assumed to be up to a few hundred metres in thickness and the permeability was calculated using the modified Blake-Korzeny Carmen equation of McKenzie (1984).

	Bulk rock	Interstitial melt	Plagioclase Ya 47	Alkali feldspar Ya 38	Amphibole Ya 2 (rim)	Biotite Ya 14
SiO_2	59.08	65.86	59.28	64.50	44.62	36.24
TiO_2	0.64	0.67	0.05	–	1.14	3.72
Al_2O_3	17.08	14.26	25.44	18.40	8.29	17.89
FeO^t	7.35	5.65	0.10	0.14	13.41	27.43
MnO	0.15	0.19	0.03	0.06	1.04	0.15
MgO	2.72	2.86	–	–	13.94	6.18
CaO	5.70	3.52	7.72	0.03	10.76	0.19
Na_2O	3.07	2.32	7.27	1.20	1.24	0.36
K_2O	2.64	4.61	0.06	14.80	0.32	7.74
Total	98.60	99.95	99.85	100.11	98.04	99.90

	Bulk rock	Interstitial melt
Density (Kg/m^3):		
1.5 wt.% H_2O:	2.48×10^3	2.40×10^3
6.0 wt.% H_2O:		2.20×10^3
Viscosity (Pa s):		
1.5 wt.% H_2O:		2.40×10^8
6.0 wt.% H_2O:		7.0×10^3
Permeability (m^2):		
50% porosity:	1.25×10^{-8}	
10% porosity:	3.0×10^{-11}	
Gravity ($m\ s^{-2}$):	9.81	
Thermal diffusivity ($m^2\ s^{-1}$):	1×10^{-7}	
Mush thickness (m):	1–500	

A study of porosity occlusion in the granodiorite sample described above has been possible because alkali feldspar underwent an additional stage of nucleation and growth as pore spaces became isolated from one another during the latter stages of solidification. An estimate based on the modal abundance of the alkali feldspar pockets suggest that the pore network became disconnected at porosities below about 3–4%. The melt remained interconnected at porosities above this, allowing alkali feldspar crystallization to continue on the rims of existing crystals. It is suggested that the crystallization of alkali feldspar exclusively on the rims of the plates while the porosity remained connected is evidence for the localised (mm-cm scale) diffusion of species within the melt phase.

Despite evidence for the interconnectivity of the pore network down to 3–4%, Rayleigh number calculations indicate that compositional convection is unlikely to have occurred during interstitial crystallization of the Yauca granodiorite. Even using the most optimistic of values gives Rayleigh numbers

several orders of magnitude lower than required for compositional convection. If there was any separation of melt from crystals in the Yauca granodiorite, it must therefore have been restricted to much higher porosities and permeabilities, i.e. before development of a touching crystal framework. The large difference between the calculated Rayleigh number and that required for compositional convection suggests that these conclusions may also apply to other granitic rocks with similar chemistry, mineralogy and texture.

References

Atherton, M.P. and Sanderson, L.M. (1985) The chemical variation and evolution of the superunits of the segmented Coastal Batholith. In *Magmatism at a plate edge: the Peruvian Andes*. (W.S. Pitcher, M.P. Atherton, E.J. Cobbing and R.D. Beckinsale, eds.). Blackie, Halstead Press, Glasgow, pp 108–18.

Beere, W. (1975) A unifying theory of the stability of penetrating liquid phases and sintering pores. *Acta Metallurgica*, **23**, 131–8.

Bottinga, Y, Richet, P. and Weill, D.F. (1983) Calculation of the density and thermal expansion coefficient of silicate liquids. *Bull. Mineral.*, **106**, 129–38.

Bryon, D.N. (1992) *Textural development in granitoid rocks: a case study from the zoned Linga superunit of the Coastal Batholith, Peru.* Unpubl. PhD thesis, Univ. of Liverpool.

Bryon, D.N., Atherton, M.P. and Hunter, R.H. (1994) The description of the primary textures of Cordilleran granitic rocks. *Contrib. Mineral. Petrol.*, **117**, 66–75.

Bryon, D.N., Atherton, M.P. and Hunter, R.H. (1995) The interpretation of granitic textures from serial thin sectioning, image analysis and three-dimensional reconstruction. *Mineral. Mag.*, **59**, 203–11.

Bulau, J.R., Waff, H. and Tyburczy, J.A. (1979) Mechanical and thermodynamic constraints of fluid distribution in partial melts. *J. Geophys. Res.*, **84**, 6102–8.

Daines, M.J. and Richter, F.M. (1988) An experimental method for directly determining the interconnectivity of melt in a partially molten system. *Geophys. Res. Letts.*, **15**, 1459–62.

Fowler, A.C. (1985) The formation of freckles in binary alloys. *IMA J. Appl. Maths.*, **35**, 159–74.

Harte, B., Hunter, R.H. and Kinny, P.D. (1993) Melt geometry, movement and crystallization in relation to mantle dykes, veins and metasomatism. *Phil. Trans. R. Soc., London.* **A342**, 1–21.

Hunter R.H. (1987) Textural equilibrium in layered igneous rocks. In *Origins of igneous layering*. (I. Parsons, ed.), pp 473–503.

Huppert, H.E. (1990) The fluid dynamics of solidification. *J. Fluid Mech.*, **212**, 209–40.

Jurewitz, S.R. and Watson, B.E. (1985) The distribution of partial melt in a granite system: The application of liquid phase sintering theory. *Geochim. Cosmochim. Acta*, **49**, 1109–21.

Laporte, D. (1988) Wetting angle between silicic melts and biotite. *Abstract. Trans. AGU*, **69**, No. 44, p. 1411.

Mahood, G.A. and Cornejo, P.C. (1992) Evidence for ascent of differentiated liquids in a silicic magma chamber found in a granitic pluton. *Trans. Royal Soc. Edin.*, **83**, 63–9.

Martin, D. (1990). Crystal settling and in situ crystallization in aqueous solutions and magma chambers. *Earth Planet. Sci. Lett.*, **96**, 336–48.

McCarthy, T.S. and Robb, L.J. (1978) On the relationships between cumulus mineralogy and trace and alkali element chemistry in an Archean granite from the Barberton region, South Africa. *Geochim. Cosmochim. Acta*, **42**, 21–6.

McKenzie, D.P. (1984) The generation and compaction of partially molten rock. *J. Petrol.*, **25**, 713–65.

Petford, N. (1993) Porous media flow in granitoid magmas: an assessment. In *Flow and Creep in the Solar System: Observations, Modelling and theory.* (D.B. Stone and S.K. Runcorn, eds.). Kluwer Academic Publishers, Netherlands, 261–86.

Ragland, P.C. and Butler, J.R. (1972) Crystallization of the West Farrington pluton, North Carolina, U.S.A. *J. Petrol.*, **13**, 381–404.

Sawka, W.N., Chappell, B.W. and Kistler, R.W. (1990) Granitoid compositional zoning by side-wall boundary layer differentiation: evidence from the Palisade Crest intrusive suite, Central Sierra Nevada, California. *J. Petrol.*, **31**, 519–53.

Shaw, H.R. (1972) Viscosities of magmatic silicate liquids: an empirical method of prediction. *Amer. J. Sci.*, **272**, 870–89.

Smith, C.S. (1948) Grains, phases, and interfaces: an interpretation of microstructure. *A.I.M.E. Trans.*, **175**, 15–51.

Sparks, R.S., Huppert, H.E. and Turner, J.S. (1985) The fluid dynamics of evolving magma chambers. *Phil. Trans. R. Soc., London*, **A310**, 511–34.

Tait, S. and Jaupart, C. (1992) Compositional convection in a reactive crystalline mush and melt differentiation. *J. Geophys. Res.*, **97**, 6735–56.

Tindle, A.G. and Pearce, J.A. (1981) Petrogenetic modelling of *in situ* fractional crystallization in the zoned Loch Doon pluton, Scotland. *Contrib. Mineral. Petrol.*, **78**, 196–207.

Worster, M.G. (1991) Natural convection in a mushy layer. *J. Fluid Mech.*, **224**, 335–59.

[*Revised manuscript received 10 July 1995*]